Configurable 3D-Printed Millifluidic and Microfluidic 'Lab on a Chip' Reactionware Devices

Philip J. Kitson, Mali H. Rosnes, Victor Sans, Vincenza Dragone, Leroy Cronin*

WestCHEM, School of Chemistry, University of Glasgow, University Avenue, Glasgow G12 8QQ, UK,

**Corresponding author email: Lee.Cronin@glasgow.ac.uk; http://www.croninlab.com*

Table of Contents

1 General Experimental Remarks

All chemical reagents and solvents were purchased from Sigma Aldrich and used without further purification.

Design Software: The 3D-printed labware used in this work was designed on the freely distributed 3D CAD software Autodesk123D (http://www.123dapp.com/) although any 3D modelling / CAD software with the ability to export models in a .STL file format would suffice for this, and there are a number of suitable alternative free / open source candidates available on the internet. The device designs were exported as .STL files (available from the authors), which was then interpreted by Bits from Bytes Axon 2 software which produces a 3D printer instruction file (.bfb file) which was subsequently transferred to the 3dTouch^{TM} 3D printer. The printing was conducted in a layer-by-layer fashion by the 3dTouch^{TM} printer, and the devices were printed using polypropylene (PP), and were subsequently fitted with standard PTFE 1/16" OD tubing and connections.

Device Setups: All solutions were pumped by means of C-3000 syringe pumps from Tricontinent equipped with 1 mL syringes. An in-house developed Labview application was employed to program the pumps to deliver the desired flow-rates and to control the UV-Vis and IR spectroscopy.

UV-Vis spectroscopy: UV-Vis spectra were acquired with a DH-2000 light source and a flow cell FIA-Z-SMA 905 (10 mm pathlength) from Ocean Optics, connected by fiber optics to a AvaSpec 2048 from Avantes. Spectra were collected every 1-2 seconds employing a customized program and processed employing an in-house developed program with Labview.

IR spectroscopy: IR spectra were collected employing a Nicolet IS-5 from Thermo Scientific and a ZnSe Golden Gate ATR from Specac equipped with a flow cell. The resolution was set at 4 cm^{-1} and 16-80 scans were recorded.

DLS: DLS spectra were recorded with a NanoZS from Malvern Scientific employing disposable cuvettes 24 hours after collection of samples.

Mass Spectrometry: The spectra were recorded using a JEOL JMS 700 (FAB / EI / CI). The observed *ca.* m/z values are listed.

Optical Microscopy: Optical microscopy was performed on a Keyence VHX-600 (Gen II) digital microscope with a 20-200x lens. 3D Channel profiles were calculated by varying the focal length of the microscope in increments of 5 microns and using the Keyence digital microscope software to compile the resulting images into a 3D plot of the channel cross-section.

NMR Spectroscopy: All NMR data were recorded on a Bruker Advance 400 MHz, in deuterated MeOH from Goss Scientific, at T = 300 K. All chemical shifts are given in ppm. The peaks are denoted s = singlet and m = multiplet.

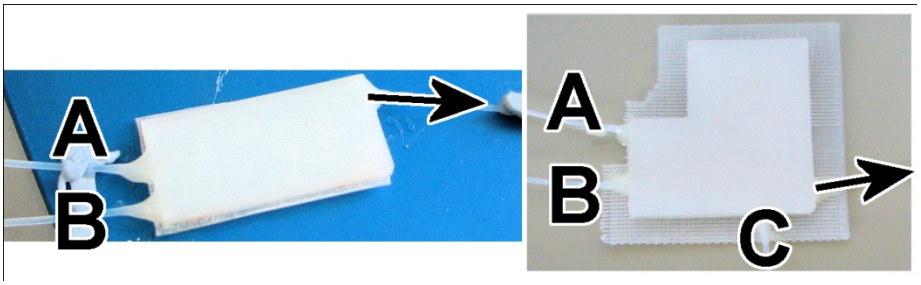

Figure S1: R1 (left) and R2 (right) indicating the various inlets and outlets.

2 Organic syntheses

2.1 Imine Synthesis

A 1 M methanolic solution of benzaldehyde (inlet B) was mixed with a 1 M methanolic solution of benzylamine (inlet A) in R1 at the same flow rate (see Figure S2). The total flow rates ranged from 10 to 200 µL min^{-1}. The outlet of the reactor was connected to the flow-cell in a Golden Gate ATR-IR machine. The products were analysed by flow ATR-IR and standard ^{1}H NMR. **^{1}H NMR**: (400 MHz, $CDCl_3$) (δ, ppm) 8.32 (s, 1H), 7.72–7.70 (m, 2H), 7.35–7.33 (m, 3H), 7.27–7.24 (m, 4H), 7.20–7.17 (m, 1H), 4.75 (s, 2H). **IR:** 1704 cm^{-1} peak from C=O moiety disappeared, 1644 cm^{-1} peak from C=N-C moiety appeared.

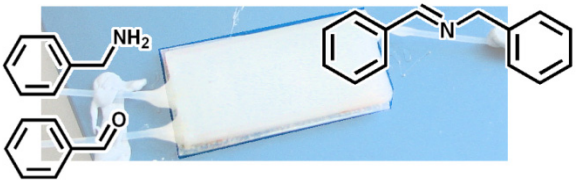

Figure S2: An overview of how R1 was used in the synthesis of the imine.

2.2 Secondary amine synthesis

A 1 M solution of benzaldehyde in MeOH was pumped through inlet B into R2 at 2.5-5 µL min^{-1} and mixed with a 1 M solution of benzylamine in MeOH introduced through inlet A at the same flow rate, allowing sufficient residence time to synthesise the corresponding imine. A reducing agent, namely cyanoborohydride (1 M), was introduced through inlet C at the same flow rate to produce the corresponding amine (see Figure S3). The samples were characterised by flow ATR-IR and MS spectroscopy. **MS**: (EI^{+}) calculated for $C_{14}H_{15}N$ (M^{+}) *m/z* 197.12, found 197.09. **IR:** 1704 cm^{-1} peak from C=O moiety disappeared, 1644 cm^{-1} peak from C=N-C moiety disappeared (see Figure S4).

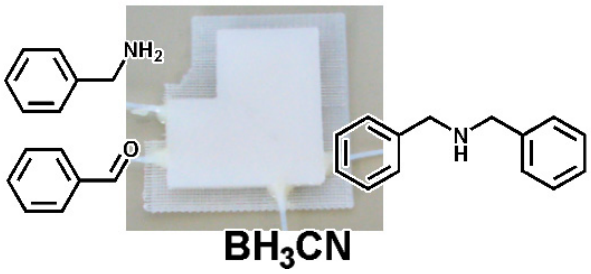

Figure S3: An overview of how R2 was used in the synthesis of the secondary amine. When inlet C is inactive the imine is formed.

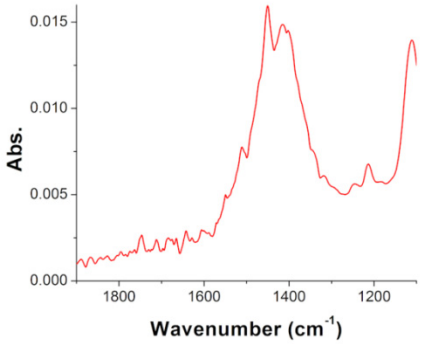

Figure S4: ATR-IR spectrum showing no absorbance related to the C=O stretch from the aldehyde moiety or the C=N-C stretch from the imine moiety, suggesting that the imine was successfully reduced to a secondary amine.

2.3 Tertiary amine synthesis

A mixture of benzaldehyde (1 M) and cyanoborohydride (1 M) (1:1) (v:v), in methanol, was introduced into R2 through inlet B at 5 µL min^{-1}. Simultaneously, a 1 M solution of benzylamine was pumped through inlet A at 2.5 µL min^{-1}. Allyl bromide (0.25 M) was employed as alkylating agent through inlet C at 7.5 µL min^{-1}. The samples were analysed by flow ATR-IR and MS spectroscopy. The results were a mixture of secondary and tertiary amines containing dibenzylamine (1), tribenzylamine (3) and the product corresponding to the alkylation of dibenzylamine allyl-dibenzyl-amine (2) (see Figure S5). **MS**: (CI^+) calculated for $C_{14}H_{15}N$ (1), $C_{17}H_{19}N$ (2) and $C_{21}H_{21}N$ (3) $[M+H]^+$ *m/z* 198.13 (1), 238.16 (2), 288.18 (3), found 198 (1), 238 (2), 288 (3).

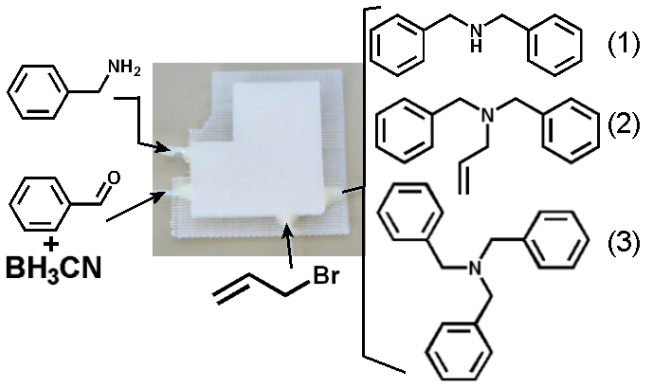

Figure S5: An overview of how R2 was used for an alkylation process. The reducing agent does not react with the aldehyde; hence the allykaltion step can take place without the introduction a fourth inlet.

3 Inorganic syntheses

3.1 {Mo_{36}} Synthesis

The synthesis of the {Mo_{36}} cluster ($[Mo_{36}O_{112}(H_2O)_{16}]^{8-}$) was successfully conducted in both R1 and R2. A 0.625 M aqueous solution of $Na_2MoO_4 \cdot 2H_2O$ was pumped through inlet A of R1 at 50 µL min^{-1}, while HCl (1 M) was pumped at the same flow rate through inlet B of R1. The product was characterised by UV-Vis spectroscopy and DLS analysis. **UV-Vis:** λ_{max} = 360 nm (see Figure S6). **DLS:** Particles of average hydrodynamic diameter of 1.5 nm were observed (see Figure S8 (left)).

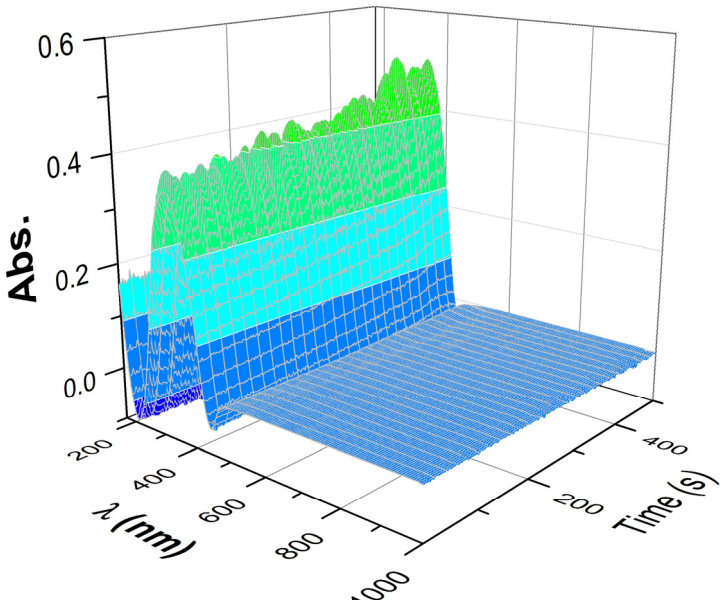

Figure S6: Time dependent UV-Vis spectra corresponding to the synthesis of {Mo_{36}}.

3.2 $\{Mo_{154}\}$ Synthesis (Molybdenum blue)

A 0.625 M aqueous solution of Na_2MoO_4 was introduced into R2 through inlet A. At the same time, a 1 M solution of HCl was introduced through inlet B. After mixing in the reaction channel, a third solution containing hydrazine (0.12 M) was introduced through inlet C. All solutions were pumped at the same flow rates. The total flow rates were 18.25, 37.5 and 75 µL min^{-1}, respectively. The product was characterised by UV-Vis spectroscopy and DLS analysis. **UV-Vis:** Main λ_{max} = 750 nm (some $\{Mo_{36}\}$ with λ_{max} = 360 nm in also present). See Figure S6. **DLS:** Particles of average hydrodynamic diameter of 3.6 nm were observed (see Figure S8 (right)).

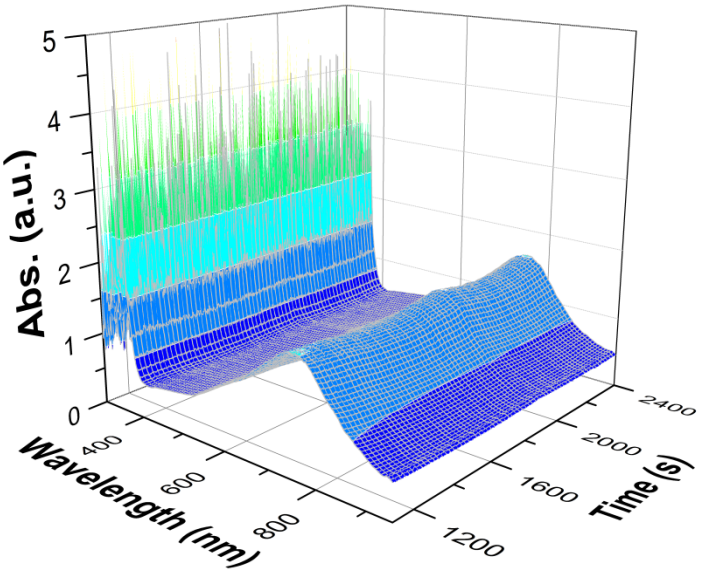

Figure S7: Time dependent UV-Vis spectra corresponding to the synthesis of $\{Mo_{154}\}$ from $\{Mo_{36}\}$. The pH of the final solutions were between 0.4 and 1.9, which is $\{Mo_{154}\}$, $\{Mo_{150}\}$ or $\{Mo_{148}\}$, or a mixture, depending on the accurate pH value.

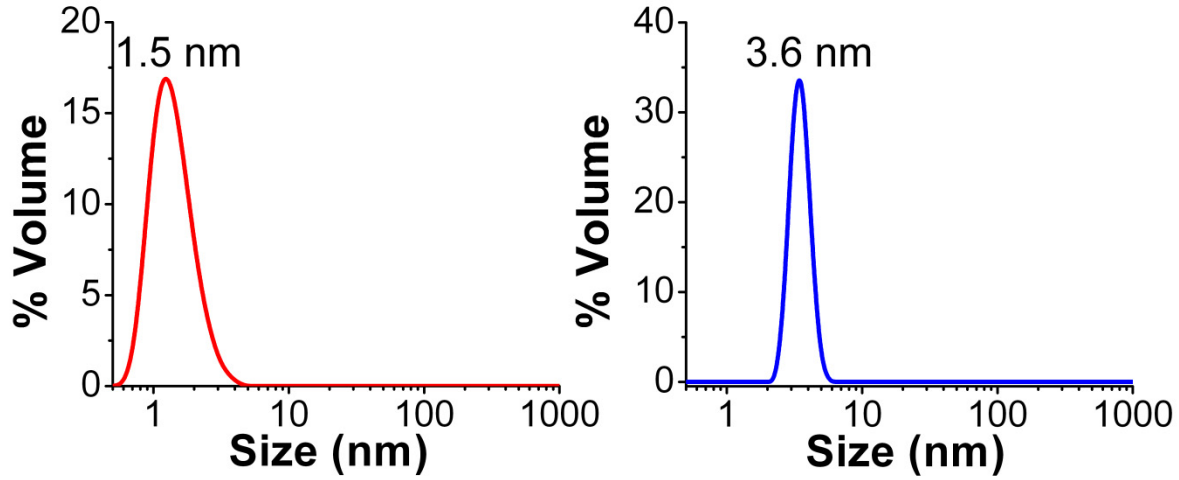

Figure S8: The hydrodynamic diameters observed from the DLS analysis; (left) $\{Mo_{36}\}$, and (right) $\{Mo_{154}\}$.

3.3 Synthesis of {Mo_{154}} using R3

During the printing of R3 the print process was paused and solid sodium molybdate ($Na_2MoO_4 \cdot 2H_2O$, 300 mg, 1.24 mmol) was added to "silo A" and hydrazine dihydrochloride ($NH_2NH_2 \cdot 2HCl$, 20 mg, 0.19 mmol) was added to "silo B", before the print process was restarted and the "silos" closed up (see Figure S9). A pH 1 solution of HCl was pumped at 25 µL min^{-1} consecutively through both chambers. The formation of {Mo_{154}} was observed in the outlet stream by off-line UV-Vis and DLS analysis.

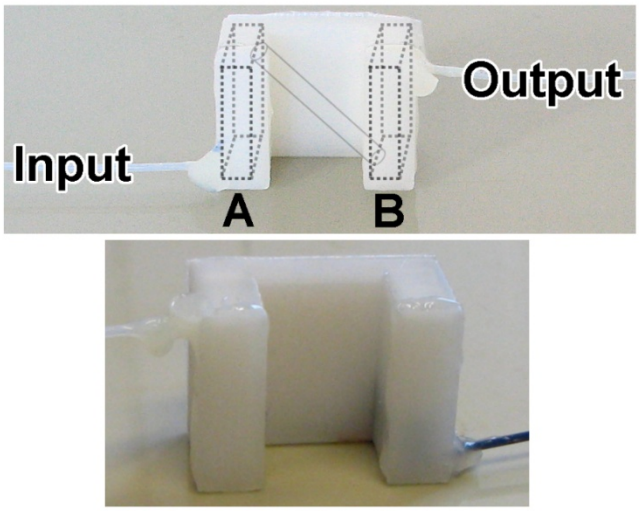

Figure S9: (top) An overview of the inlet, silos A and B, and the outlet. (bottom) The bottom of silo B and the outlet have turned blue indicating the presence of molybdenum blue.

4 The synthesis of gold nanoparticles

R1 was employed in this synthesis. A (1:1) mixture of aqueous solutions of $HAuCl_4$ (0.2 mM) and sodium citrate (2 mM) was pumped through inlet A at 50-60 µL min^{-1}, while an aqueous solution of sodium borohydride (10 mM) was pumped through inlet B at the same flow rate. The synthesis was followed by flow UV-Vis spectroscopy. The absorbance intensity of the gold nanoparicles decreased over time probably due to the deposition of gold on the reactor walls (see Figure S10). **UV-Vis:** λ_{max} = 537 nm. **DLS:** Particles of average hydrodynamic diameter of 10.1 nm were observed.

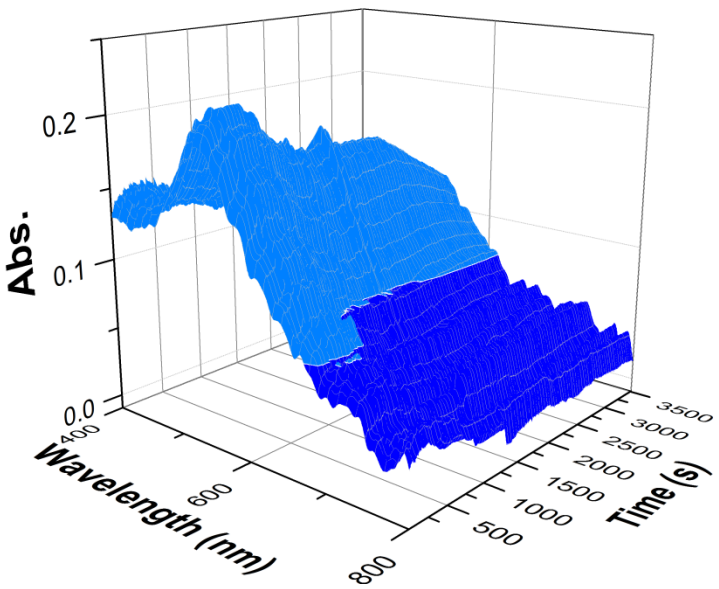

Figure S10: Time dependant UV-Vis data showing how the intensity of the absorption maxima of the gold nanoparticles decreased over time.